Turbocharged SI Engine Models for Control

Jamil El Hadef, Guillaume Colin, Yann Chamaillard, Vincent Talon

Turbocharged SI Engine Models for Control

J. El Hadef[(1)(2)], G. Colin[(1)], Y. Chamaillard[(1)] and V. Talon[(2)]
[(1)] University of Orleans, [(2)] Renault SAS

Laboratoire PRISME, 8 rue Leonard de Vinci
45000 Orleans cedex 2, FRANCE
Phone : 0033 (0)2 38 49 43 83
E-mail: jamil.el-hadef@etu.univ-orleans.fr

Turbocharging penetration is forecast to increase in the next few years. The additional complexity will usually be tackled by a growth of the use of simulations in the product development cycle. It includes validations and calibrations on virtual test benches as well as model-based control laws.

A 0D model, designed to be embedded directly into a predictive control law is presented in this paper. Its steady-state and transients performances are presented and compared to the results obtained with a reference simulator built on a commercial software. Both models well capture the engine dynamic through the entire operating range but with regard to the implementation effort that is needed, each of them stay dedicated to its current application.

Topics / Spark-Ignited Engine Modeling, Turbocharger Modeling, Air Path Control

1. INTRODUCTION

Severe pollutant emission standards constrain to reduce the fuel consumption and pollutant emissions of internal combustion engines. Downsized engines appear to be the car manufacturers privileged way in terms of emission reduction as well as investment minimization. In this context, turbocharging represent a major possibility to maintain the performances of small displacement engines.

The increase of complexity can be tackled using model-based control strategies [1, 2]. They include validation and pre-calibration on virtual test-bench but also control laws with an embedded model. A virtual test bench model requires being accurate while for the second one a low calculation time is fundamental. For these reasons, in both cases, 0D models are preferred against 1D or 3D modeling.

In this paper, two models are presented. The first one has been designed to be embedded in a model predictive control strategy. It is based on physical equations and data-map calibrated from steady-state test bench measurements exclusively. A second model, which can be used as a virtual test bench, is then presented. It relies on the LMS AMESim commercial software library and has also been calibrated using steady-state data points.

Both models include a compressor and a turbine sub-model based on extrapolated data-map. In fact, the turbocharger manufacturers do not provide any information at low rotational speed (typically under 80,000 rpm). In this study, an innovative extrapolation strategy based on physics has been used to build the data-map. This study confirms the great performances expected in [3].

2. SYSTEM DESCRIPTION

The engine used for the study is a 1.2L turbocharged spark-ignited engine. In such an engine, the intake flow pressure is increased by a compressor before being cooled down through a heat exchanger. Finally, the actual cylinders inlet flow is controlled using a variable flow restriction called throttle. At the exhaust, a by-pass known as wastegate, allows controlling the amount of gas which passes through the turbine. The latter directly drives the intake compressor by recovering energy from the exhaust gas (see figure 1).

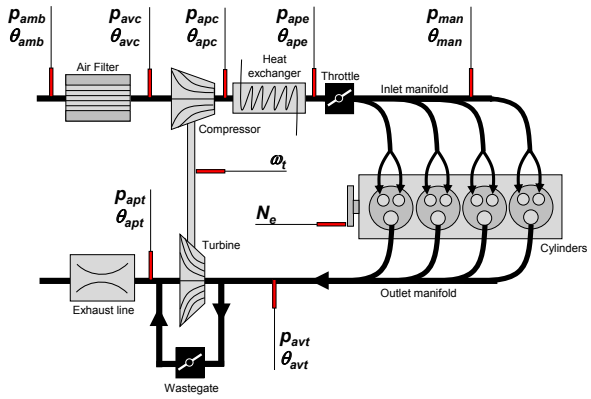

Fig. 1. Engine test bench sensors configuration used for the study (p stands for pressure, θ for temperature N_e and ω_t are respectively the engine and turbocharger rotational speed). Throttle position is recorded while wastegate position is estimated.

An engine test bench as well as a vehicle has been used to acquire respectively steady-state data and transients. Actuators positions as well as different physical quantities including various pressures and temperatures were recorded (see figure 1).

3. EMBEDDED CONTROL MODEL

The embedded control model must combine accuracy and stability while keeping a low calculation time. Moulin et al. [4] stated that, for this purpose, a 0D approach combined with a mean value cylinders model is the most appropriate.

In such models, each control volume of the air path is followed by a flow restriction, itself followed by another control volume (see figure 2). The pressure in each volume is taken as a state of the model. Its dynamic is governed by a differential equation which links the derivative of the pressure to the inlet and outlet flow rates and temperatures.

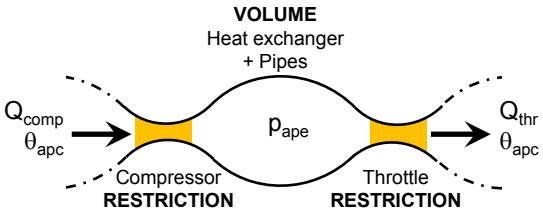

Fig. 2. Example of a succession of control volumes and restrictions: the heat exchanger and its pipes are surrounded by two flow restrictions: the compressor and the throttle.

The flow rate at the inlet (respectively at the outlet) depends on the area of the flow restriction at the entrance (respectively at the exit) of each volume. For the compressor and the turbine, the flow rate is directly read in data-map.

All together, the model contains three control volumes: the inlet and outlet manifold and the heat exchanger. It respectively corresponds to three state: p_{man}, p_{avt} and p_{apc} (see figure 1).

3.1 Pressures and temperatures computation

The differential equation which governs the pressure dynamic in the control volume is deduced from Euler's mass, energy and momentum equations. Under the assumption of constant temperature in the given volume V, this equation is given by [5]:

$$\frac{\partial p}{\partial t} = \frac{\gamma r}{V}\left(Q_{m_{in}}\theta_{in} - Q_{m_{out}}\theta_{out}\right) \tag{1}$$

where p is the pressure, γ is the ratio of specific heats, r is the fluid gas constant, Q_m the mass flow rate and θ the temperature. Indices *"in"* and *"out"* respectively stand for inlet and outlet of the considered control volume.

The dynamic of the temperature is supposed to be much slower than the pressure one. Such a hypothesis leads to calculate the temperature in each reservoir through an algebraic relation which depends on the considered volume. Each of them will be detailed in a case-by-case basis in the following sub-sections.

3.2 Throttle and wastegate models

The throttle and wastegate effects are estimated using a flow restriction model. Supposing it is compressible and isentropic, the flow can be computed using the pressures on each side of the orifice [6, 7] by:

$$\begin{cases} Q_m = \frac{p_{us}}{\sqrt{r\theta_{us}}} S\sqrt{\gamma}\left(\frac{2}{\gamma+1}\right)^{\frac{\gamma+1}{2(\gamma-1)}} & if \quad \frac{p_{ds}}{p_{us}} \geq \left(\frac{2}{\gamma+1}\right)^{\frac{\gamma}{\gamma-1}} \\ Q_m = \frac{p_{us}}{\sqrt{r\theta_{us}}} S\left(\frac{p_{ds}}{p_{us}}\right)^{\frac{1}{\gamma}}\sqrt{\frac{2\gamma}{\gamma-1}\left(1-\left(\frac{p_{ds}}{p_{us}}\right)^{\frac{\gamma-1}{\gamma}}\right)} & otherwise \end{cases} \tag{2}$$

where S is the effective area of the orifice. The indices *"us"* and *"ds"* respectively stand for upstream and downstream.

3.3 Engine air mass flow rate

To describe the flow rate entering the engine we multiply the theoretical flow rate at inlet manifold conditions by a correction factor. It takes into account the actual ability of the engine to aspire air from the intake manifold [4, 6]. This factor is called volumetric efficiency and calibrated using steady-state test bench measurements:

$$Q_{eng} = \frac{p_{man}V_{cyl}}{r\theta_{man}}\frac{N_e}{120} \times \eta_{vol}\left(\frac{p_{man}}{\theta_{man}}, N_e\right) \tag{3}$$

where Q_{eng} is the engine flow rate, p_{man} and θ_{man} the manifold pressure and temperature, V_{cyl} the engine displacement, N_e the engine rotational speed and η_{vol} a volumetric efficiency nonlinear function which is usually approximated using a second order polynomial, a look-up table or a neural network.

3.4 Cylinders exhaust mass flow rate and temperature

At the exhaust, the flow rate is the sum of the engine mass flow rate described above Q_{eng} and the fuel mass flow rate Q_{fuel} injected in the cylinders.

When modelling turbocharged engine, a peculiar attention must be paid to the exhaust gas temperature θ_{avt}. In fact, it represents the energy that can be recovered by the turbine as well as influences the intake flow rate. It is usually linked to the inlet manifold gas temperature as well as the exhaust flow rate [8]:

$$\theta_{avt} = \theta_{man} + k_{ech}\frac{Q_{fuel}\times LHV}{C_p(Q_{fuel}+Q_{eng})} \tag{4}$$

where LHV is the lower heating value, C_p the specific heat at constant pressure and k_{ech} represents the proportion of the total energy which is transferred to the flow at the exhaust:

$$k_{ech} = \Phi_{k_{ech}}(N_e, Q_{fuel}, Q_{eng}) \tag{5}$$

where $\Phi_{k_{ech}}$ is a nonlinear function usually approximated by a second order polynomial, a look-up table or a neural network calibrated on steady state test bench measurements.

3.5 Turbocharger model

3.5.1 Compressor sub-model

The compressor mass flow rate is directly read in a data-map $\Phi_{Q_{comp}}$ inverted and extrapolated from the operating points provided by the manufacturer:

$$Q_{comp} = \Phi_{Q_{comp}}(\pi_c, \omega_t) \tag{6}$$

where Q_{comp} is the compressor outlet mass flow rate, π_c the compression ratio $\left(\pi_c = \frac{p_{apc}}{p_{avc}}\right)$ and ω_t the turbocharger rotational speed.

The extrapolation methodology is fully detailed in [3] and summed up in paragraph 5.

The outlet flow temperature depends on the compressor isentropic efficiency η_{comp}:

$$\theta_{apc} = \theta_{amb}\left(\frac{\pi_c^{\frac{\gamma-1}{\gamma}}-1}{\eta_{comp}}+1\right) \quad (7)$$

where θ_{apc} is the temperature downstream the compressor, θ_{amb} the atmospheric temperature and η_{comp} the compressor isentropic efficiency directly read in an extrapolated data-map $\Phi_{\eta_{comp}}$:

$$\eta_{comp} = \Phi_{\eta_{comp}}(Q_{comp}, \omega_t) \quad (8)$$

3.5.2 Turbine sub-model

The turbine mass flow rate Q_{turb} is read in an extrapolated data-map $\Phi_{Q_{turb}}$:

$$Q_{turb} = \Phi_{Q_{turb}}(\pi_t, \omega_t) \quad (9)$$

where π_t is the expansion ratio $\left(\pi_t = \frac{p_{avt}}{p_{apt}}\right)$.

The flow temperature at the outlet of the turbine, θ_{turb}, is given by:

$$\theta_{turb} = \theta_{avt}\left[1-\eta_{turb}\left(1-\left(\frac{1}{\pi_t}\right)^{\frac{\gamma-1}{\gamma}}\right)\right] \quad (10)$$

where θ_{avt} is the outlet manifold temperature and η_{turb} the turbine isentropic efficiency read in a data-map $\Phi_{\eta_{turb}}$:

$$\eta_{turb} = \Phi_{\eta_{turb}}(\pi_t, \omega_t) \quad (11)$$

3.5.3 Turbocharger rotational speed computation

The compressor and the turbine are mechanically linked. A fourth state equation is needed to describe the turbocharger dynamic through its rotational speed ω_t [4]:

$$\dot{\omega_t} = \frac{1}{I}\left(T_{turb} - T_{comp} - T_f\right) \quad (12)$$

where I is the turbocharger inertia, T_{turb} and T_{comp} respectively represent the turbine and compressor torques and T_f is the shaft friction torque which is usually neglected.

Compressor and turbines torques depend on the mass flow rate, the inlet and outlet temperature and the turbocharger rotational speed:

$$T_{comp} = \frac{Q_{comp}\times C_p\times(\theta_{apc}-\theta_{amb})}{\omega_t} \quad (13)$$

$$T_{turb} = \frac{Q_{turb}\times C_p\times(\theta_{avt}-\theta_{turb})}{\omega_t} \quad (14)$$

4. VIRTUAL TEST BENCH MODEL

4.1 Modelling strategy

The model was built using the LMS AMESim commercial software. This type of model is usually easy to implement but require a certain calibration experience.

In the sketch (see figure 3), all the components are taken from libraries included in the software. In particular, the model uses the "Mean Value Engine Model" block which contains a volumetric efficiency data-map (see equation 3). It has directly been built using steady-state operating points recorded on the test bench. The other significant elements of this model are the compressor and turbine sub-models which essentially rely on four data map.

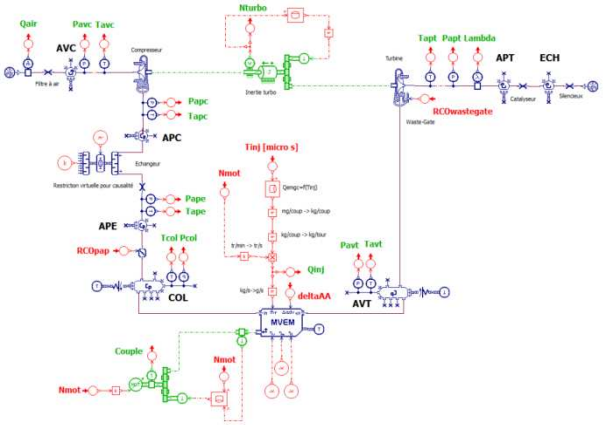

Fig. 3. AMESim engine model sketch.

The model is calibrated using exclusively steady state test bench measurements. It is validated on those operating points as well as on vehicle transients. Performances are detailed in paragraph 6.

4.2 Model description

4.2.1 Air filter, catalyst and muffler

The intake air filter and the exhaust line (catalyst and muffler) are simulated using flow restriction model. Orifice area and flow coefficient are constants calibrated using the steady-state test bench measurements.

4.2.2 Actuators

The throttle and wastegate are also simulated using flow restrictions. For the first one, the effective area with respect to the actuator position is well known. It is directly implemented as a 1D data-map and the flow coefficient is set to 1. For the wastegate, the maximum area is geometric. The flow coefficient is estimated using a PI controller on the inlet manifold pressure. No model for the actuators dynamic is implemented.

4.2.3 Heat exchanger

To simulate the heat exchanger effect, the best compromise is to use the combination of a standard heat exchanger and a flow restriction. It allows modelling respectively the temperature and pressure drops that is experimentally observed on the test bench.

4.2.4 Turbocharger

The compressor and turbine components both rely on two data-map which links pressure ratio, flow rate, efficiency and rotational speed. These data-map are directly extrapolated from manufacturer's steady state data points. The method is described in the next paragraph. Thanks to the good accuracy of the data-map extrapolation, only one correction factor is required for the turbine efficiency data-map. This coefficient helps to take into account the heat transfer that occurs between the turbine and the compressor but that are not taken into account in the extrapolation method.

5. TURBOCHARGER DATA-MAP EXTRAPOLATION

With downsized engines, the accuracy at low turbocharger rotational speeds (typically lower than 80,000 rpm) is essential. However, manufacturers usually provide no points at such operating conditions. As a consequence, an efficient extrapolation strategy is necessary to build the data-map that are required in the turbocharger sub-models.

Popular extrapolation methods are usually not based on physical equations but empirical observations [9, 10, 11]. Recently, a new physics-based method has been developed in order to tackle the extrapolation to low rotational speed with more accuracy and robustness [3, 10]. It is described below.

5.1 Compressor data-map extrapolation

Using the head parameter Ψ and the dimensionless flow rate Φ lead to a simplified physical relationship between pressure ratio, flow rate and rotational speed:

$$\Psi = \frac{A(\omega_t)+B(\omega_t)\Phi}{C(\omega_t)-\Phi} \tag{15}$$

where A, B and C are 1D data map. The identification uses a Levenberg-Marquardt algorithm and manufacturer's data points. For the interpolation, monotone piecewise cubic interpolation should be used [13, 14, 15].

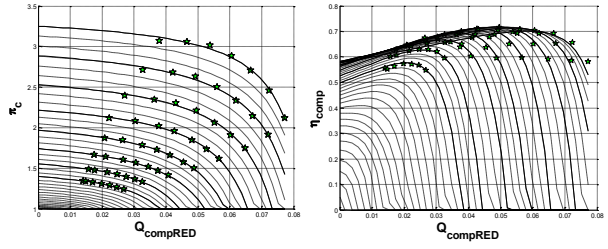

Fig. 4. Compressor pressure ratio (on the left) and efficiency (on the right). Extrapolation results are plotted (solid lines) as well as the manufacturer points (stars). $Q_{compRED}$ is the normalized compressor air mass flow rate.

The isentropic efficiency of the compressor η_{comp} (see figure 4) is calculated as the ratio of the isentropic specific enthalpy exchange Δh_{is} and the specific enthalpy exchange Δh:

$$\eta_{comp} = \frac{\Delta h_{is}}{\Delta h} \tag{16}$$

The first one is directly calculated using the head parameter definition while the other one is described by a linear equation with respect to the flow rate [10, 12]:

5.2 Turbine data-map extrapolation

The turbine usually acts as nothing more than an adiabatic nozzle on the flow rate. It can then be described using the standard equation of compressible gas flow [4]:

$$Q_{turbRED} = S \times V_{ns} \tag{17}$$

where $Q_{turbRED}$ is the normalized turbine mass flow rate [8, 16], S the equivalent section and V_{ns} the normalized flow speed which depends on the flow state (subsonic or supersonic, see (9)).

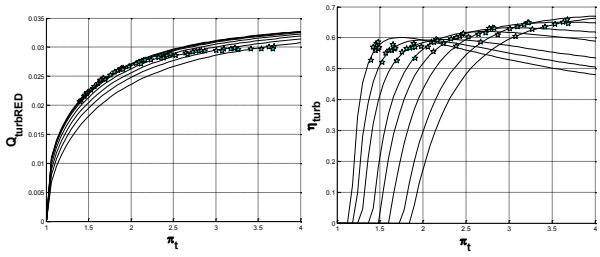

Fig. 5. Turbine reduced flow rate (on the left) and efficiency (on the right). Extrapolation results are presented (solid line) as well as manufacturer points (stars).

The improvement proposed in [3] relies on a new way to describe the evolution of the section, based on the most recent experimental observations:

$$S = k_1 \times \left(1 - e^{\left(1-\frac{1}{\pi_t}\right)^{k_2(\omega_t)}}\right) \tag{18}$$

where k_1 is a constant and k_2 a second order polynomial with respect to the rotational speed. Parameters are directly identified on the data provided by the manufacturer.

For the turbine isentropic efficiency (see figure 5) the method is similar to the compressor one:

$$\eta_{turb} = \frac{\Delta h}{\Delta h_{is}} \tag{19}$$

The specific enthalpy exchange is computed using a linear relationship [10, 12] under the hypotheses of a constant fluid density [17]. The isentropic specific enthalpy exchange only depends on the pressure ratio so no effort is needed at this point.

6. RESULTS AND DISCUSSION

6.1 Steady-state validation

For both models, the calibration process exclusively rely on steady-state test bench measurements. As a consequence, these points represent the first set of validation data. Performances for pressures, temperatures, air mass flow rate and turbocharger rotational speed estimations are depicted in figures 6 to 9.

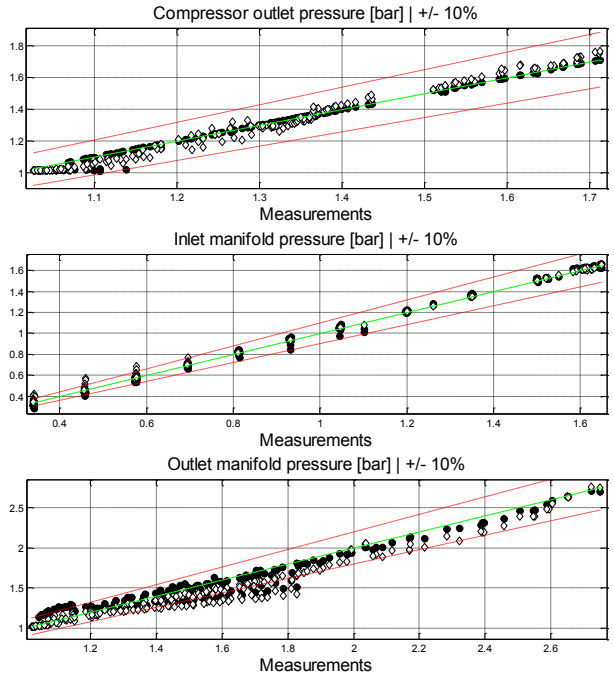

Fig. 6. Pressures estimation performance for the reference simulator (white diamonds) and for the embedded control model (black dots). Correlation lines are plotted : a perfect model would give 45 degrees tilted straight line.

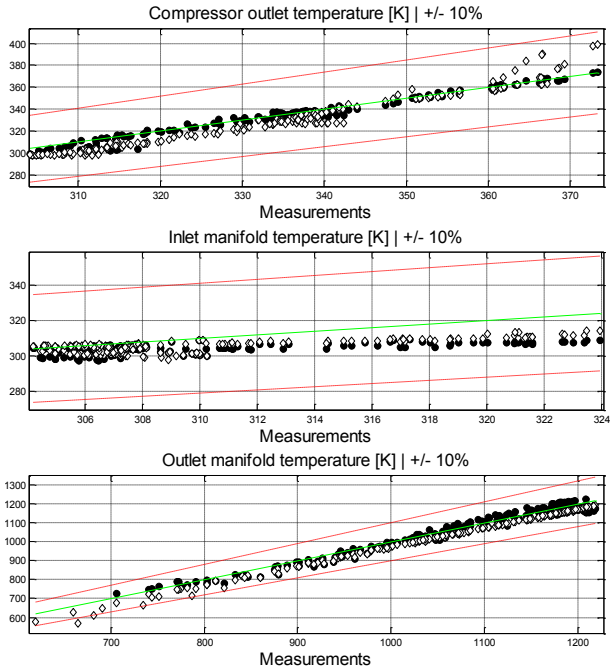

Fig. 7. Temperatures estimation performance for the reference simulator (white diamonds) and for the embedded control model (black dots).

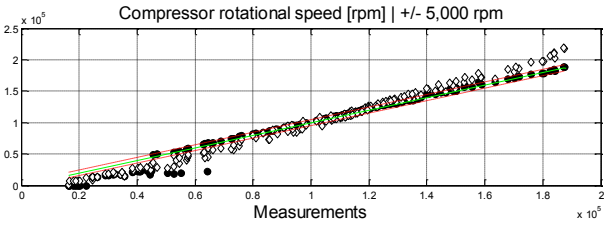

Fig. 8. Turbocharger rotational speed estimation performance for the reference simulator (white diamonds) and for the embedded control model (black dots).

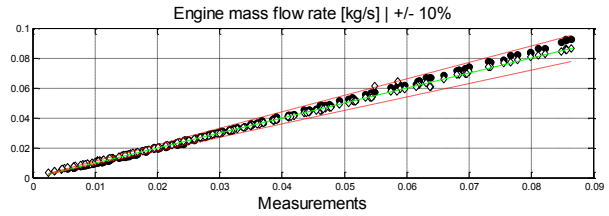

Fig. 9. Air mass flow rate estimation performance for the reference simulator (white diamonds) and for the embedded control model (black dots).

6.2 Vehicle transient validation

The purpose of the study is to investigate the performances of two models, built on two different platforms but both dedicated to be use in a control law synthesis process. As such, the dynamic of the system must be perfectly estimated through the whole engine operating range.

Models performances are illustrated in figures 10 and 11 for the four states of the model, i.e. compressor outlet pressure, inlet and outlet manifold pressures and turbocharger rotational speed. During the transient, engines speed varies from 2,000 to 6,000 rpm while throttle and wastegate opening ranges are fully explored.

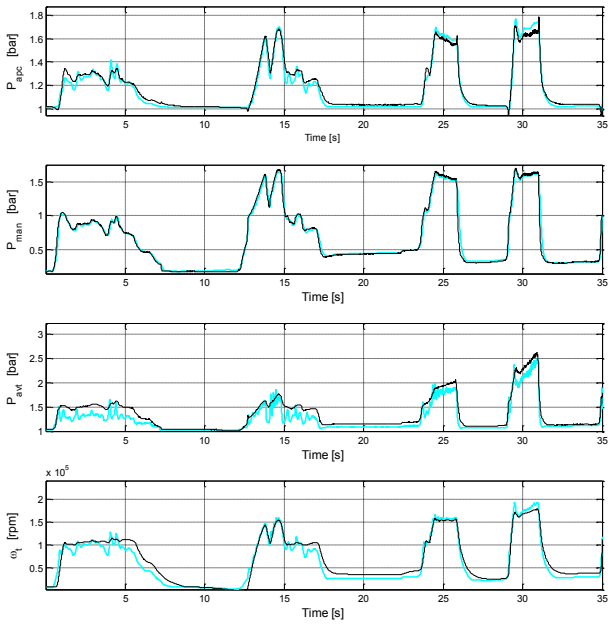

Fig. 10. Vehicle transient validation for the virtual test bench model (thin line: measurements – thick line: reference simulator estimation).

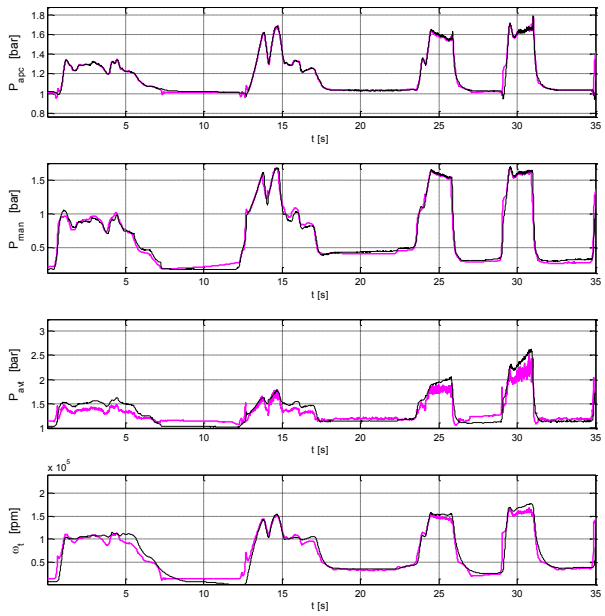

Fig. 11. Vehicle transient validation for the embedded control model (thin line: measurements – thick line: embedded control model estimation).

6.3 Discussion

On figures 6 to 11, it can be seen that the behavior of both models is similar. The error on steady-state quantities is very low. For the embedded control model, it rarely exceeds 5% except for the outlet manifold pressure, which for, the average error is about 10%. For the reference simulator model, the error is a bit higher but still remains acceptable. For both models, the temperature is very well estimated using algebraic relationships.

Concerning the estimation of the turbocharger rotational speed (see figure 8), the error reaches 25,000 rpm for the embedded control model and 30,000 rpm for the virtual test bench model. Although the maximum errors are analogous, the average of the first one is much lower. High rotational speeds are also better estimated with the first model.

On vehicle transient, the behavior is again similar for both models (see figures 10 and 11). The dynamic is well captured for the four states of the model. This is crucial when talking about control purposes. The value error is really low for three of the four states but again, a highest relative error is reached in the estimation of the outlet manifold pressure.

7. CONCLUSION

The global steady-state and transient performances of the models are presented side by side and compared. The conclusion is that they both present a high accuracy with respect to the implementation and calibration effort that is required. As a consequence, they are perfect candidates for an industrial control strategy synthesis.

To improve the robustness of a control law which would use one of these models, one should consider adding actuator models. Here, the models have been validated using measured or estimated actual positions.

REFERENCES

[1] Dauron, A., *Model-Based Powertrain control: Many Uses, No Abuse*, Oil & Gas Science and Technology - Rev. IFP Energies nouvelles, 62, 2007, 427-435.

[2] Guzzella, L. et al., *Introduction to Modeling and Control of Internal Combustion Engine Systems*, Springer, 2004.

[3] El Hadef, J. et al., *Physical-Based Algorithms for Interpolation and Extrapolation of Turbocharger Data Maps*, SAE Int. J. Engines, 5, 2012.

[4] Moulin, P. et al., *Modelling and Control of the Air System of a Turbocharged Gasoline Engine*, Proc. of the IFAC World Conference 2008, 2008.

[5] Hendricks, E., *Isothermal versus Adiabatic Mean Value SI Engine Models*, 3rd IFAC Workshop, Advances in Automotive Control, 2001, 373-378.

[6] Heywood, J. B., *Internal Combustion Engines Fundamentals*, McGraw-Hill, 1988.

[7] Talon, V., *Modélisation 0-1D des Moteurs à Allumage Commandé,* Université d'Orléans, 2004.

[8] Eriksson, L., *Modeling and Control of Turbocharged SI and DI Engines*, Oil & Gas Science and Technology - Rev. IFP Energies nouvelles, 62, 2007, 523-538.

[9] Jensen, J.-P. et al., *Mean Value Modeling of a Small Turbocharged Diesel Engine*, SAE, 1991.

[10] Martin, G. et al., *Physics Based Diesel Turbocharger Model for Control Purposes*, SAE, 2009.

[11] Moraal, P. et al., *Turbocharger Modeling for Automotive Control Applications*, SAE, 1999.

[12] Martin, G. et al., *Implementing Turbomachinery Physics into Data-Map Based Turbocharger Models*, SAE, 2009.

[13] Draper, N. R. et al., *Applied Regression Analysis* Third, Wiley, 1998.

[14] Fritsch, F. N. et al., *Monotone Piecewise Cubic Interpolation*, SIAM Journal on Numerical Analysis, 17, 1980.

[15] Walter, E. et al., *Identification of Parametric Models from Experimental Data*, Springer, Londres, 1997.

[16] Eriksson, L. et al., *Modeling of a Turbocharged SI Engine*, Annual Reviews in Control, 26, 2002, 129-137.

[17] Vitek, O. et al., *New Approach to Turbocharger Optimization using 1-D Simulation Tools*, SAE Technical Paper, 2006-01-0438, 2006.